Head and Neck Pathology (2022) 16:158–167
https://doi.org/10.1007/s12105-022-01418-9

PROCEEDING OF THE NORTH AMERICAN SOCIETY OF HEAD AND NECK PATHOLOGY COMPANION MEETING, MARCH 20, 2022, LOS ANGELES, CA

Proceedings of the North American Society of Head and Neck Pathology, Los Angeles, CA, March 20, 2022. Emerging Bone and Soft Tissue Neoplasms in the Head and Neck Region

Bin Xu[1]

Received: 30 October 2021 / Accepted: 18 January 2022 / Published online: 21 March 2022

Abstract
In the past decade, several emerging bone and soft tissue neoplasms of the head and neck region have been described in the literature, including *GLI1*-altered mesenchymal tumors, (intraosseous) rhabdomyosarcoma with *TFCP2* fusion, and adamantinoma-like Ewing sarcoma. This review provides a summary of the clinical features, histologic characteristics, immunoprofile, key diagnostic features, and differential diagnoses of these emerging entities. Notably, all three entities show epithelioid morphology and cytokeratin immunopositivity, highlighting the need to consider these mesenchymal neoplasms in the differential diagnoses of cytokeratin-positive epithelioid tumors in the head and neck region. Appropriate workups including detection of the characteristic molecular alterations are essential for the correct diagnosis.

Keywords *Gli1*-altered mesenchymal tumor · Spindle/sclerosing rhabdomyosarcoma · Rhabdomyosarcoma with *TFCP2* rearrangement · Adamantinoma-like Ewing sarcoma · Ewing sarcoma · Ectomesenchymal chondromyxoid tumor

Introduction

For the past several years, several emerging bone and soft tissue tumors have been described in the literature, all of which have a propensity to occur in the head and neck region. Such entities include *GLI1*-altered mesenchymal tumors, (intraosseous) rhabdomyosarcoma with *TFCP2* fusion, and adamantinoma-like Ewing sarcoma. In this review, we summarized the clinical presentation, histologic features, immunoprofile, diagnostic molecular alterations, differential diagnoses, and diagnostic pitfalls of these emerging entities.

✉ Bin Xu
xub@mskcc.org

[1] Department of Pathology and Laboratory Medicine, Memorial Sloan-Kettering Cancer Center, 1275 York Avenue, New York, NY 10065, USA

GLI1-Altered Mesenchymal Tumors

In 2004, Dahlen et al. first described *GLI1* translocation in a distinct soft tissue neoplasm initially named as "pericytoma with t(7;12) translocation". This tumor was originally proposed to be of pericytic differentiation based on its ultrastructural characteristics and its smooth muscle actin (SMA)-positive/S100-negative immunoprofile [1]. However, multiple recent studies published since 2019 have shown that *GLI1*-altered mesenchymal tumors have a more variable immunoprofile with frequent S100 and CD56 positivity, which argue against the purported pericytic origin [2–5]. At present time, these tumors are best regarded as mesenchymal tumors of an uncertain lineage of differentiation.

Two distinct mutually-exclusive *GLI1*-alterations have been reported in these tumors: first being *GLI1* translocation with fusion partners including *ACTB, PTCH1, MALAT1*, *APOD*, and *DERA*; and the second being *GLI1* amplification often with co-amplification and protein overexpression of nearby genes, including *DDIT3, CDK4, MDM2*, and/or *STAT6* [4–7]. The underlying molecular alterations do not appear to affect histologic findings and clinical outcomes [4].

Clinical Presentation and Outcome

GLI1-altered mesenchymal tumors affect patients of a wide age range from 1-year-old to 79-year-old, with a median age of presentation of 37 years [1–5, 8]. There is no obvious sex predilection. Approximately 40% occur in the head and neck region [4]. Among head and neck *GLI1*-altered tumors, 70 to 80% occur in the tongue [1, 3–5]. Other anatomic sites that may be involved include the submandibular gland [4], neck soft tissue [4], soft palate [9], and hypopharynx (unpublished case, Fig. 1).

Although the initially reported cases followed a benign course after complete excision, later reports have shown that these tumors have malignant potential with the risk of regional and distant metastasis being 5% and 20% respectively [2–5]. Among the reported cases of *GLI1*-altered tumors in the head and neck region, only those located outside of the oral tongue have been associated with metastasis [4].

Histologic Characteristics and Immunoprofile

At low magnification, *GLI1*-altered mesenchymal tumors typically have a multinodular to plexiform growth pattern (Fig. 1). Protrusion of a tumor into vascular spaces was a common histologic finding, being seen in over 70% of the cases. At high power, the tumor is composed of monomorphic tumor cells with round to ovoid nuclei and clear to eosinophilic cytoplasm arranged in a distinctive nested, zellballen-like, to trabecular architectures separated by a rich delicate arborizing vascular network.

The mitotic activity is variable, ranging from nil to over 10 per 10 high power fields. Uncommon histologic findings that may be the presence of a small subset of tumors include the presence of focal myxoid to hyalinized stroma, tumor necrosis, prominent cell spindling with fascicular

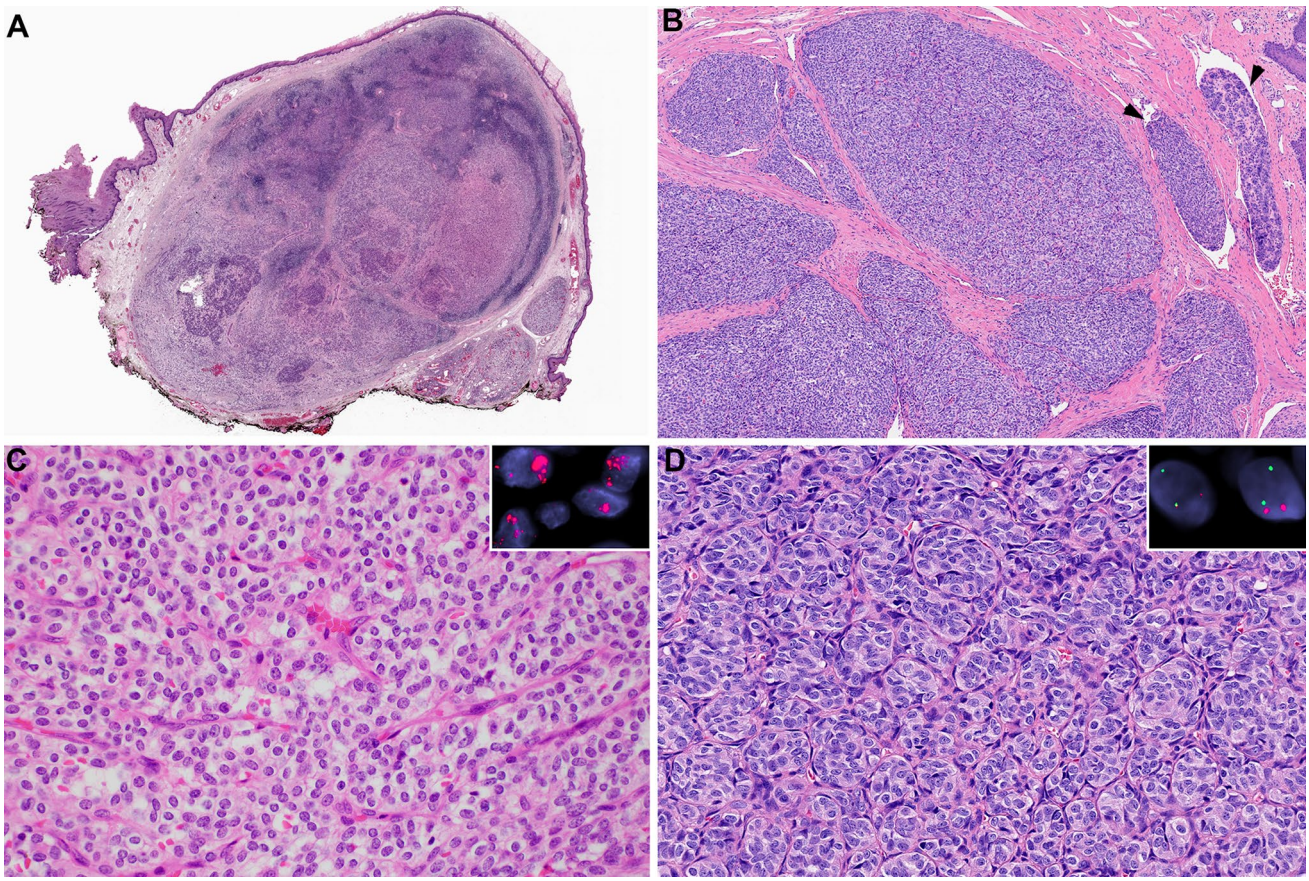

Fig. 1 *GLI1*-altered mesenchymal tumors. **A** and **C** A hypopharyngeal tumor with *GLI1* amplification. Insert: fluorescence in situ hybridization (FISH) shows *GLI1* amplification (red signal). **B** and **D** A tongue tumor with *ACTB::GLI1* translocation. Insert: FISH study using *GLI1* break-apart probes (red: centromeric; green: telomeric) demonstrates the presence of *GLI1*-translocation. At low power, GLI1-altered mesenchymal tumors show multinodular **A** to plexiform, **B** growth patterns. Vascular protrusion of a tumor (arrowheads) is a frequent histologic finding. At high power, the tumor cells have bland oval nuclei, clear (**C**) to eosinophilic (**D**) cytoplasm, and are arranged as trabeculae or nests separated by a rich delicate branching capillary network

arrangement, microcystic, pseudoglandular, and/or pseudorosette architecture. These uncommon features, when present, are often focal and accompanied by areas with the typical histologic features as described above and in Fig. 1.

The immunoprofile of *GLI1*-altered tumors is quite variable. The most frequent positive immunohistochemical markers include CD56 (in approximately 60% of cases), S100, and SMA (in over 40% of cases, Fig. 2) [2–10]. Other stains that have been reported to be positive in a small proportion of these tumors include epithelial membrane antigen (EMA), Neuron-Specific Enolase (NSE), CD10, D2-40, CD99, and H-caldesmon. Cytokeratin AE1/AE3 is positive in approximately 15% of cases. They are typically negative for synaptophysin, chromogranin, SOX10, glial fibrillary acidic protein (GFAP), desmin, myogenin, melan-A, HMB45, CD34, and p63. *GLI1*-amplified tumors may show overexpression of CDK2, MDM2, or STAT6 [4, 5].

Differential Diagnoses

The main differential diagnoses for *GLI1*-altered mesenchymal tumor in the head and neck region include paraganglioma, neuroendocrine tumor, ectomesenchymal chondromyxoid tumor, and salivary gland neoplasms, especially those with myoepithelial differentiation. The key differences among these tumors are summarized in Table 1.

Ectomesenchymal Chondromyxoid Tumor (EMCMT)

EMCMT is a rare mesenchymal tumor of uncertain histogenesis that typically occurs in the anterior dorsal tongue [11, 12]. Rare cases have also been reported in extra-glossal locations, such as the gingiva, palate, tonsils, and mandible [13].

EMCMT and *GLI1*-altered mesenchymal tumors share a certain histologic similarity, including a propensity for oral tongue location, multilobulated growth pattern, and immunopositivity for S100, SMA, and keratins.

However, several histologic differences may distinguish these two entities. Cytologically, the tumor cells of EMCMT typically are spindle to stellate (Fig. 3), although epithelioid cells with round nuclei may also present focally; whereas *GLI1*-altered tumors typically have an epithelioid cytomorphology with clear cytoplasm. Furthermore, EMCMT lacks

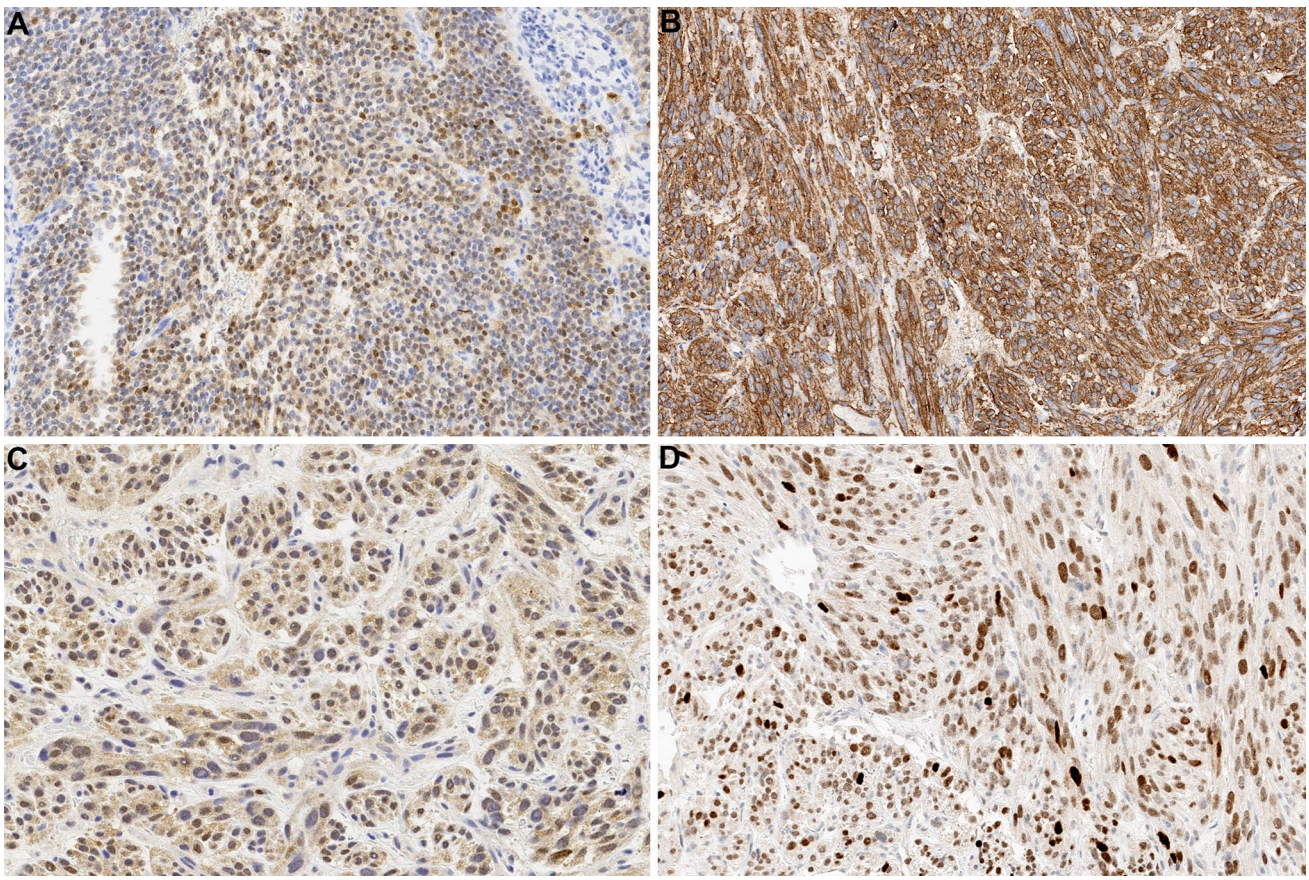

Fig. 2 Immunoprofile of GLI1-altered mesenchymal tumors. These tumors are frequently positive for S100 (**A**) and SMA (**B**). The GLI1-amplified subset may show overexpression of MDM2 (**C**) and CDK4 (**D**)

Table 1 Differential diagnoses for *GLI1*-altered mesenchymal tumors

	GLI1-altered mesenchymal tumor	Ectomesenchymal chondromyxoid tumor	Paraganglioma (PG) and neuroendocrine tumor (NET)	Salivary gland neoplasms with myoepithelial differentiation
Location	Common: tongue Other sites: submandibular gland, palate, hypopharynx, neck	Common: anterior dorsal tongue Other sites: gingiva, tonsil, mandible and palate	Broad distribution: upper aerodigestive tract, salivary gland, middle ear, and carotid body	Major and minor salivary glands
Histologic features				
Growth pattern	Multinodular to plexiform	Multinodular	Non-specific	Non-specific. Myoepithelial carcinoma may show expansile nodular growth
Delicate arborizing vascular network	Present	Absent	Present	Absent
Nested architecture	Present	Absent	Present	Absent
Stroma	Usually absent. Focal myxoid to hyalinized stroma is present in 20%-30% cases	Present: myxoid, fibrotic, or hyalinized. Chondroid stroma may present in rare cases	Absent	Myxoid to hyalinized stroma is present in certain subtypes
Immunohistochemistry				
Cytokeratin AE1/AE3	Positive in 15% of cases	Commonly positive	NET: positive PG: negative	Positive
S100	Commonly positive	Commonly positive	NET: typically negative PG: positive in sustentacular cells	Commonly positive in myoepithelial component
SMA	Commonly positive	Commonly positive	Negative	Commonly positive in myoepithelial component
CD56	Commonly positive	May be positive	Positive	Negative
Synaptophysin and chromogranin	Typically negative	Negative	Positive	Negative
Molecular alterations	*GLI1* translocation or amplification	*RREB1::MKL2* translocation Small percentage has *EWSR1* translocation	NET: Unknown PG: a subset has germline *SDHB* mutations	Varies based on diagnosis Myoepithelial carcinoma: *PLAG1* or *HMGA2* fusion

the characteristic arborizing delicate capillary network and nested architecture of *GLI1*-altered mesenchymal tumors. Myxoid to hyalinized stroma is a prominent feature of EMCMT, whereas most *GLI1*-altered tumors lack a stromal component. At the molecular level, approximately 90% of EMCMTs harbor *RREB1::MKL2* fusion, whereas a small percentage (< 5%) have *EWSR1* fusion [11].

Clinically, nearly all reported EMCMTs follow a benign clinical course. None has distant or regional metastasis. One reported case shows locally aggressive features with bone invasion [13].

Paraganglioma and Well-Differentiated Neuroendocrine Tumor

Given the epithelioid cytomorphology, the prominent nested/zellballen-like architecture, the rich capillary network, and the CD56 immunopositivity, *GLI1*-altered tumors bear certain histological resemblance to a paraganglioma or a well-differentiated neuroendocrine tumor (carcinoid tumor and atypical carcinoid tumor). The most useful immunohistochemistry studies to distinguish between these entities are a combination of S100, synaptophysin, and chromogranin. S100 is commonly positive in *GLI1*-altered tumors either diffusely or focally in a non-sustentacular pattern, whereas it highlights the sustentacular network in paraganglioma and is negative in a neuroendocrine tumor. Synaptophysin and chromogranin, markers that are diffusely positive in paragangliomas and neuroendocrine tumors, but are negative in all but one *GLI1*-altered mesenchymal tumor [9]. In equivocal cases, molecular testing for *GLI1* alterations is essential for the correct diagnosis.

Salivary Gland Neoplasms

A small percentage (20–30%) of *GLI1*-altered mesenchymal tumors may contain a focal area of a stromal component, either myxoid or hyalinized. The presence of a stromal component, together with the S100 and SMA immunopositivity, may raise concern for a salivary gland neoplasm, especially

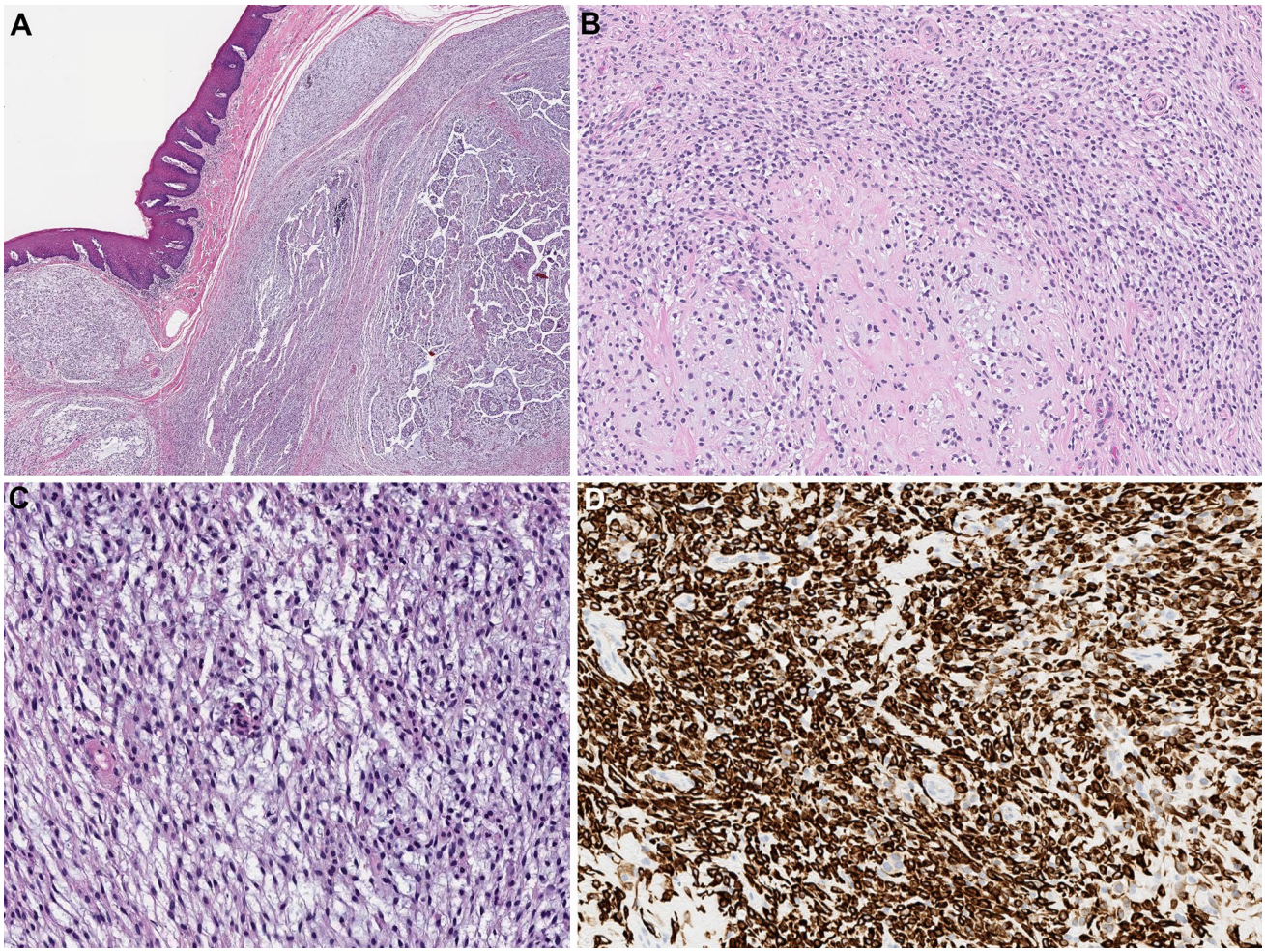

Fig. 3 An ectomesenchymal chondromyxoid tumor of the anterior dorsal tongue with *RREB1-MKL2* fusion. **A** At low power, the tumor shows a multinodular growth pattern. **B** The tumor is composed of monotonous bland spindle cells arranged as loose fascicles. whirling and a hyalinized to myxoid stroma is present. **C** The tumor cells are arranged in a reticular pattern in a myxoid background. **D** The tumor is diffusely positive for GFAP

those with stromal component or those with myoepithelial differentiation, such as pleomorphic adenoma, myoepithelioma, myoepithelial carcinoma, and adenoid cystic carcinoma. The distinction between the two relies on the presence of typical nested architecture and branching capillary network, the lack of typical features of a salivary gland neoplasm, and the identification of *GLI1* alteration in GLI1-altered mesenchymal tumors.

In conclusion, *GLI1*-altered mesenchymal tumors are characterized by a propensity of oral tongue location, a nested architecture separated by a delicate branching capillary network, an epithelioid cytomorphology with clear to eosinophilic cytoplasm, frequent immunopositivity for S100, SMA, and CD56, and the presence of *GLI* fusion or amplification. The *GLI1*-amplified tumors may additionally show co-amplification and/or overexpression of CDK4, MDM2, and/or STAT6.

Rhabdomyosarcoma with *TFCP2* Fusion

Rhabdomyosarcoma with *TFCP2* fusion is a newly described subtype of rhabdomyosarcoma that typically occurs intraosseously [14–18]. In the 5th edition of WHO classification of tumors of soft tissue and bone (2020) [19], rhabdomyosarcoma with *TFCP2* fusion is classified as a subtype of spindle cell/sclerosing rhabdomyosarcoma. Recent molecular advances detect several unique molecular alterations in spindle cell/sclerosing rhabdomyosarcoma, including rearrangements involving *TFCP2, VGLL2, NCOA2*, and *CITED2,* and *MYOD1*-mutations [19]. Among them, rhabdomyosarcoma with *TFCP2* fusion has a striking propensity to the head and neck region, especially the craniofacial bone [14–18].

The fusion partners for *TFCP2* are *FUS* in two-third of cases, and *EWSR1* in the remaining tumors.

Clinical Presentation and Outcome

Rhabdomyosarcoma with *TFCP2* fusion most commonly affects patients in their young adulthood but may occur in pediatric and elderly patients (median age of presentation: 25 years, range: 11 to 85 years). Within the head and neck region, the tumor is usually originated from craniofacial bones, most commonly the mandible, followed by the maxilla and skull [14–18]. Over 95% of the reported cases are intra-osseous, although a rare case (< 5%) affecting the superficial soft tissue of the neck region has also been reported [14].

Rhabdomyosarcoma with *TFCP2* fusion of the head and neck region has a dismal outcome with risk of both lymphatic and hematogenous spread. Based on the limited follow-up data in the literature, the risk of regional lymph node metastasis and distant metastasis were approximately 20% and 50% respectively [14]. The two-year disease-specific survival is approximately 35% [14].

Histologic Characteristics and Immunoprofile

Typically, rhabdomyosarcoma with *TFCP2* fusion shows a combined epithelioid and spindle cytomorphology (Fig. 4). The spindle cells form intervening fascicles, whereas the epithelioid cells are arranged as single cells, cords, loose clusters, or solid sheets. Rhabdoid cells with eccentric nuclei and abundant glassy eosinophilic cytoplasm may be seen. True rhabdomyoblasts with cross-striation (i.e. strap cells) are generally absent. A small percentage of tumors may show a pure spindle, pure epithelioid, or round cell morphology.

Immunohistochemically, these tumors typically show evidence of myogenic differentiation. The reported rate of immunopositivity for MyoD1, myogenin, and desmin ranges from 84 to 100%. Notably, myogenin immunopositivity is generally limited compared with MyoD1, being seen in rare tumor cells or focally in 70% of cases, and negative in 16% of cases.

Characteristically, approximately 90% of rhabdomyosarcoma with *TFCP2* fusion show diffuse immunopositivity for cytokeratin AE1/AE3 and overexpression of ALK (Fig. 4). Other high and low molecular weight cytokeratins, including CK7, CAM5.2, and CK5/6, may also be positive in this tumor.

Differential Diagnosis

As most rhabdomyosarcomas with TFCP2 fusion have an epithelioid morphology, as well as diffuse and strong keratin (including high molecular weight keratin) positivity, the main differential diagnosis is a carcinoma, in particular, a spindle cell squamous cell carcinoma (sarcomatoid carcinoma), especially when soft tissue and/or mucosal involvement is present. The presence of mucosal dysplasia as well as in situ and/or invasive squamous cell carcinoma is the most useful histologic feature to gear the diagnosis towards spindle cell squamous cell carcinoma [20]. In the absence of surface dysplasia and conventional squamous cell carcinoma, the distinction between a spindle cell squamous cell carcinoma and a rhabdomyosarcoma with *TFCP2* fusion relies on a combination of immunohistochemistry studies for myogenin and MyoD1, ALK overexpression, and molecular studies for *TFCP2* translocation. Although 2% to 28% of spindle cell squamous cell carcinoma can show desmin immunopositivity, all reported spindle cell carcinomas are negative for myogenin [20–22].

In summary, rhabdomyosarcoma with *TFCP2* fusion is a newly described subtype of spindle/sclerosing rhabdomyosarcoma with a propensity for craniofacial bone, such as the mandible and maxilla. It is characterized by epithelioid and spindle cytomorphology, diffuse immunopositivity for cytokeratin, and ALK overexpression. The absence of surface dysplasia and conventional squamous cell carcinoma, as well as the presence of myogenin/MyoD1 immunopositivity and *FUS::TFCP2* or *EWSR1::TFCP2* fusion are essential to distinguish this tumor from a spindle cell squamous cell carcinoma.

Adamantinoma-Like Ewing Sarcoma (ALES)

Adamantinoma-like Ewing sarcoma is currently considered as a variant of Ewing sarcoma characterized by the presence of t(11;22) *EWSR1::FLI1* translocation and epithelial differentiation at histological, immunohistochemical, and ultrastructural levels [19, 23–26].

In 1999, ALES was first described by Bridge et al. In this initial report, all three cases occurred in the long bone of lower extremities [23]. It was not until 2008 when the first case of head and neck ALES was described in the neck soft tissue [27]. Since then, over 30 cases of ALES have been reported in the literature. Among them, approximately 75% occur in the head and neck region [24–26].

Clinical Presentation and Outcome

The median age of presentation of head and neck ALES is 36 years. However, the tumor may be seen in a wide range group from 7-year-old to 77-year-old. There is no apparent sex predilection. Within the head and neck region, all reported cases occur at extra-skeletal sites. The involved organs in descending order of frequency are the parotid gland, the thyroid gland, sinonasal tract, submandibular gland, and soft tissue of the neck and orbital region.

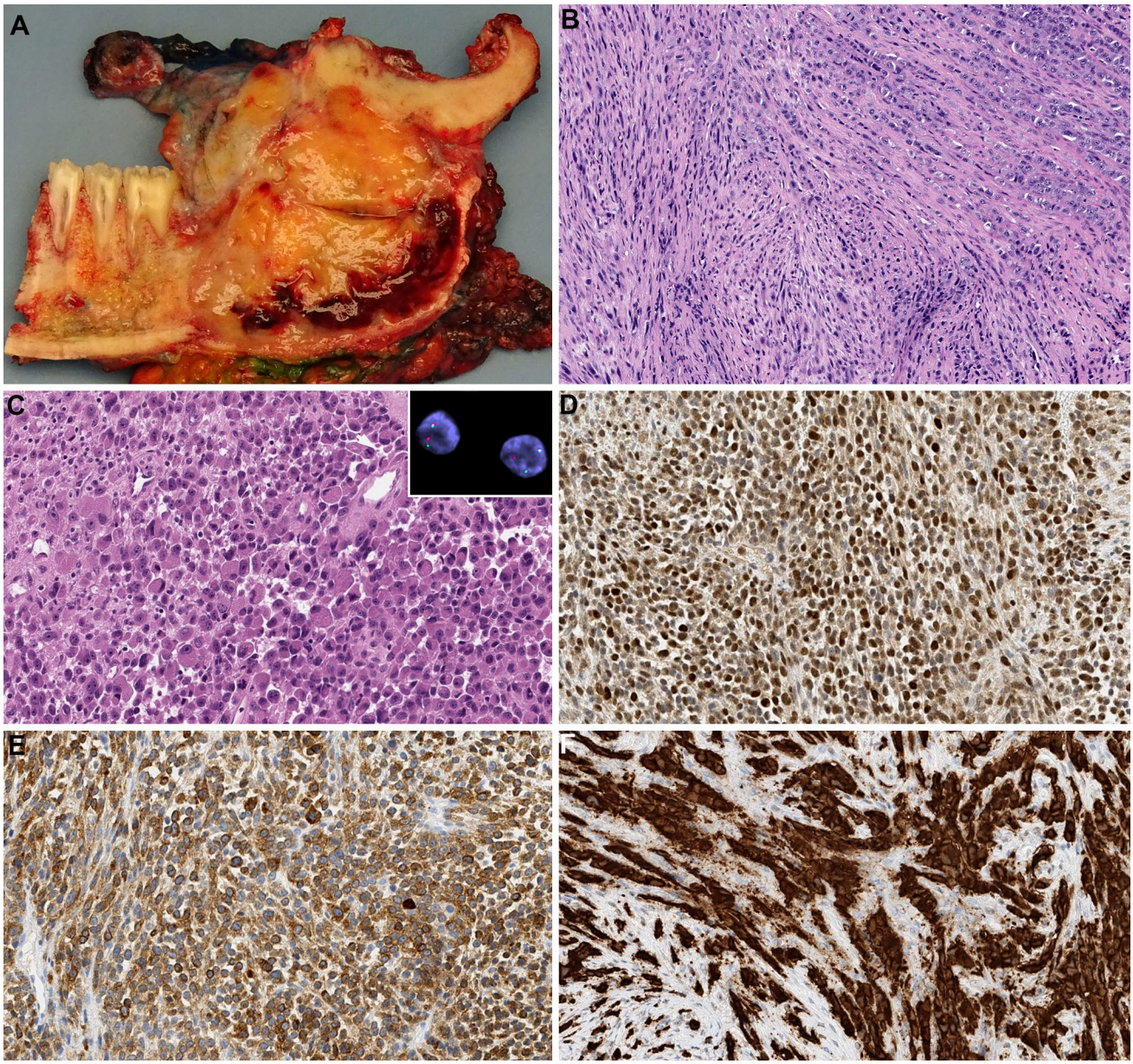

Fig. 4 An intraosseous rhabdomyosarcoma of the mandible with *TFCP2* fusion. **A** Macroscopically, the tumor is located at the angle of the mandible with bone destruction and soft tissue extension. **B** The tumor typically contains spindle cells (left) and epithelioid cells (top right). The spindle cells form fascicles, whereas the epithelioid cells are arranged as cords. **C** Rhabdoid cells with eccentric nuclei and abundant glassy eosinophilic cytoplasm may be seen. Insert: Fluorescence in situ hybridization using *TFCP2* break-apart probes demonstrates the presence of *TFCP2* translocation (separated red and green signals). (D-E) Rhabdomyosarcoma with *TFCP2* fusion is typically positive for MyoD1 (**D**), ALK (**E**), and cytokeratin AE1/AE3 (**F**)

The follow-up data for all reported head and neck ALES are scanty with short follow-up duration. To date, 12% developed distant metastasis and 6% died with the disease. One patient had a sinonasal ALES developed dural metastasis and eventually died with her disease [26], whereas the other was a 36-year-old patient with a thyroid ALES metastatic to the pancreas [28].

Given the universal expression of cytokeratin and squamous markers, there is an ongoing debate whether ALES represents a true sarcoma or a carcinoma with *EWSR1::FLI1* fusion [19, 24]. When occurring in deep soft tissue and bone as initially described by Bridge et al. [23], It is undoubtful that these tumors are best classified as sarcoma with epithelial differentiation. However, later studies, especially those

that originated in the head and neck region, documented ALES at sites in which carcinoma prevails and sarcoma is extremely rare, such as the thyroid gland and the salivary gland [24–26]. Indeed, thyroid tumors with the exact histologic features, immunoprofile, and molecular findings have also been reported as "carcinoma of the thyroid with Ewing family tumor elements (CEFTE)" [29]. At present, these tumors are classified under the umbrella of Ewing sarcoma in the WHO classification [19], even though that ALESs in the head and neck regions appear to have an improved outcome compared to the classic Ewing sarcoma, especially when the tumors arise in the thyroid and salivary glands. Additional studies on prognosis and response to Ewing sarcoma-related chemotherapy regimens are needed to eventually solve this debate.

Histologic Characteristics and Immunoprofile

Similar to the prototypical Ewing sarcoma, ALESs also show a small round cell cytomorphology (Fig. 5). The tumors cells are monotonous with a round to oval nuclei, scanty cytoplasm and inconspicuous to small nuclei, arranged as solid sheets and small nests in a fibrous, fibromyxoid, to hyalinized background. Because of the high nuclear to cytoplasmic ratio, ALESs often have a basaloid appearance. Mitotic activity and tumor necrosis are common. The tumor is highly infiltrative. Thyroid ALESs may show folliculotropism with extensive permeation of the thyroid follicles (Fig. 5C). Compact keratin pearls, peripheral palisading, rosette formation, and involvement of surface mucosa have been reported.

To date, all reported cases of ALES show diffuse and strong membranous staining of CD99 (Fig. 5D) and nuclear expression of NKX2.2. Additionally, ALESs are universally positive for pan-cytokeratin AE1/AE3 (Fig. 5E), high molecular weight cytokeratin, cytokeratin 5/6, p63, and p40 (Fig. 5F). The immunoexpression of neuroendocrine markers, including synaptophysin and chromogranin, is more variably, being detected in 57% and 20% of cases, more frequently in a focal rather than diffuse pattern. Focal S100 immunopositivity is reported in approximately 20% of ALES [24–26].

Differential Diagnosis

Given the round cell and basaloid histologic features and universal immunopositivity for cytokeratins (including high molecular weight cytokeratins), p63, and p40, the key differential diagnosis of ALES is epithelial tumors. The actual differential diagnoses are broad and vary by the sites of origin, including basaloid carcinoma (such as basal cell adenocarcinoma, high grade adenoid cystic carcinoma, and basaloid salivary duct carcinoma) and myoepithelial carcinoma in the salivary gland; anaplastic carcinoma, poorly differentiated carcinoma and intrathyroidal thymic carcinoma of the thyroid gland, and malignant small blue round cell tumors (such as melanoma, small and large cell neuroendocrine carcinoma, basaloid squamous cell carcinoma, rhabdomyosarcoma, lymphoma, and high grade olfactory neuroblastoma) in the sinonasal tract [24–26].

It is pertinent to perform immunohistochemistry for CD99 and NKX2.2 as the surrogate immunomarkers for any high grade and/or basaloid neoplasm originate from the head and neck region. Strong and diffuse CD99 membranous immunopositivity or diffuse nuclear staining of NKX2.2 should trigger subsequent confirmative molecular testing to determine the status of *EWSR1::FLI1* fusion [30].

Conclusions

In this review, we summarize the clinical behaviors, histologic features, immunoprofile, and differential diagnosis of several emerging mesenchymal tumors, including *GLI1*-altered mesenchymal tumors, (intraosseous) rhabdomyosarcoma with *TFCP2* fusion, and adamantinoma-like Ewing sarcoma. All three entities have a strong predilection to the head and neck region and may show cytokeratin positivity, including expression of high molecular weight cytokeratins in rhabdomyosarcoma with TFCP2 fusion and adamantinoma-like Ewing sarcoma. The presence of typical histologic features and immunoprofile are essential to trigger appropriate molecular testing. The detection of diagnostic molecular alterations, such as *GLI1*-amplification or fusion, *TFCP2* fusion, and *EWSR1::FLI1* fusion, is essential for the correct diagnosis.

Authors Contributions Not applicable.

Funding Research reported in this publication was supported in part by the Cancer Center Support Grant of the National Institutes of Health/National Cancer Institute under award number P30CA008748.

Data Availability Not applicable.

Code Availability Not applicable.

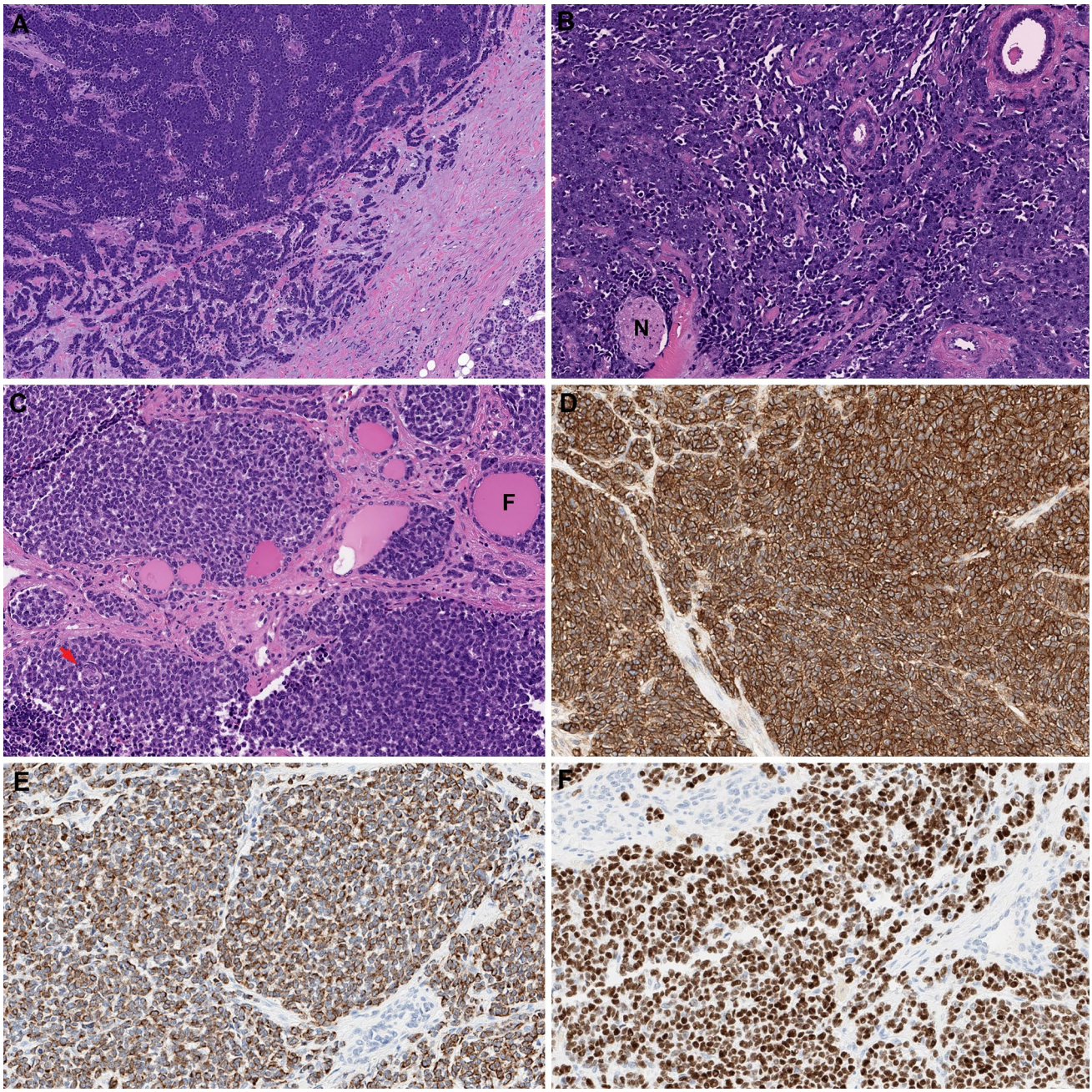

Fig. 5 Adamantinoma-like Ewing sarcoma (ALES). (**A** and **B**) An ALES of the submandibular gland. At low power (**A**), tumor cells are arranged as infiltrative cords and solid sheets in a fibrotic to sclerosing stroma. **B** The tumor is composed of monotonous small round cells. The high nuclear to cytoplasmic ratio gives a basaloid appearance. Perineural invasion (N) and infiltration among native salivary ducts are seen. **C** to **F** An ALES of the thyroid gland presents as a small round cell tumor with uniform nuclei and scanty cytoplasm infiltrating among and colonizing thyroid follicles (**F**). Tight keratin pearls (red arrows) may be seen in ALES. The tumor is positive for CD99 in a membranous pattern (**D**). Cytokeratin AE1/AE3 (**E**) and p40 (**F**) are also diffusely positive

Declarations

Conflict of interest No competing financial interests exist for the contributing author.

Ethical Approval Not applicable.

Research Involved in Human and Animal Rights Not applicable.

Consent to Participate Not applicable.

Consent for Publication Not applicable.

References

1. Dahlen A, Fletcher CD, Mertens F, Fletcher JA, Perez-Atayde AR, et al. Activation of the GLI oncogene through fusion with the beta-actin gene (ACTB) in a group of distinctive pericytic neoplasms: pericytoma with t(7;12). Am J Pathol. 2004;164:1645–53.
2. Kerr DA, Pinto A, Subhawong TK, Wilky BA, Schlumbrecht MP, et al. Pericytoma With t(7;12) and ACTB-GLI1 Fusion: Reevaluation of an Unusual Entity and its Relationship to the Spectrum of GLI1 Fusion-related Neoplasms. Am J Surg Pathol. 2019;43:1682–92.
3. Antonescu CR, Agaram NP, Sung YS, Zhang L, Swanson D, et al. A distinct malignant epithelioid neoplasm with GLI1 gene rearrangements, frequent S100 protein expression, and metastatic potential: expanding the spectrum of pathologic entities with ACTB/MALAT1/PTCH1-GLI1 Fusions. Am J Surg Pathol. 2018;42:553–60.
4. Xu B, Chang K, Folpe AL, Kao YC, Wey SL, et al. Head and neck mesenchymal neoplasms with GLI1 gene alterations: a pathologic entity with distinct histologic features and potential for distant metastasis. Am J Surg Pathol. 2020;44:729–37.
5. Agaram NP, Zhang L, Sung YS, Singer S, Stevens T, et al. GLI1-amplifications expand the spectrum of soft tissue neoplasms defined by GLI1 gene fusions. Modern Pathol. 2019;32:1617–26.
6. Nitta Y, Takeda M, Fujii T, Itami H, Tsukamoto S, et al. A case of pericytic neoplasm in the shoulder with a novel DERA-GLI1 gene fusion. Histopathology. 2021;78:466–9.
7. Lopez-Nunez O, Surrey LF, Alaggio R, Herradura A, McGough RL, et al. Novel APOD-GLI1 rearrangement in a sarcoma of unknown lineage. Histopathology. 2021;78:338–40.
8. Bridge JA, Sanders K, Huang D, Nelson M, Neff JR, et al. Pericytoma with t(7;12) and ACTB-GLI1 fusion arising in bone. Hum Pathol. 2012;43:1524–9.
9. Klubíčková N, Kinkor Z, Michal M, Baněčková M, Hájková V, et al., (2021) Epithelioid soft tissue neoplasm of the soft palate with a PTCH1-GLI1 Fusion: a case report and review of the literature. Head and Neck Pathol
10. Dahlen A, Mertens F, Mandahl N, Panagopoulos I. Molecular genetic characterization of the genomic ACTB-GLI fusion in pericytoma with t(7;12). Biochem Biophys Res Commun. 2004;325:1318–23.
11. Dickson BC, Antonescu CR, Argyris PP, Bilodeau EA, Bullock MJ, et al. Ectomesenchymal chondromyxoid tumor: a neoplasm characterized by recurrent RREB1-MKL2 fusions. Am J Surg Pathol. 2018;42:1297–305.
12. Smith BC, Ellis GL, Meis-Kindblom JM, Williams SB. Ectomesenchymal chondromyxoid tumor of the anterior tongue. Nineteen cases of a new clinicopathologic entity. Am J Surg Pathol. 1995;19:519–30.
13. Bubola J, Hagen K, Blanas N, Weinreb I, Dickson BC, et al. Expanding awareness of the distribution and biologic potential of ectomesenchymal chondromyxoid tumor. Head Neck Pathol. 2021;15:319–22.
14. Xu B, Suurmeijer AJH, Agaram NP, Zhang L, Antonescu CR. Head and neck rhabdomyosarcoma with TFCP2 fusions and ALK overexpression: a clinicopathological and molecular analysis of 11 cases. Histopathology. 2021;79:347–57.
15. Le Loarer F, Cleven AHG, Bouvier C, Castex MP, Romagosa C, et al. A subset of epithelioid and spindle cell rhabdomyosarcomas is associated with TFCP2 fusions and common ALK upregulation. Modern. 2020;33:404–19.
16. Agaram NP, Zhang L, Sung YS, Cavalcanti MS, Torrence D, et al. Expanding the spectrum of intraosseous rhabdomyosarcoma: correlation between 2 distinct gene fusions and phenotype. Am J Surg Pathol. 2019;43:695–702.
17. Watson S, Perrin V, Guillemot D, Reynaud S, Coindre JM, et al. Transcriptomic definition of molecular subgroups of small round cell sarcomas. J Pathol. 2018;245:29–40.
18. Dashti NK, Wehrs RN, Thomas BC, Nair A, Davila J, et al. Spindle cell rhabdomyosarcoma of bone with FUS-TFCP2 fusion: confirmation of a very recently described rhabdomyosarcoma subtype. Histopathology. 2018;73:514–20.
19. (2020) WHO Classification of Tumours Editorial Board. WHO classification of tumours of soft tissue and bone. World Health Organiz Classif Tumours
20. Prieto-Granada CN, Xu B, Alzumaili B, Al Rasheed MRH, Eskander A, et al. Clinicopathologic features and outcome of head and neck mucosal spindle cell squamous cell carcinoma. Virchows Arch. 2021;479:729–39.
21. Thompson LD, Wieneke JA, Miettinen M, Heffner DK. Spindle cell (sarcomatoid) carcinomas of the larynx: a clinicopathologic study of 187 cases. Am J Surg Pathol. 2002;26:153–70.
22. Viswanathan S, Rahman K, Pallavi S, Sachin J, Patil A, et al. Sarcomatoid (spindle cell) carcinoma of the head and neck mucosal region: a clinicopathologic review of 103 cases from a tertiary referral cancer centre. Head Neck Pathol. 2010;4:265–75.
23. Bridge JA, Fidler ME, Neff JR, Degenhardt J, Wang M, et al. Adamantinoma-like Ewing's sarcoma: genomic confirmation, phenotypic drift. Am J Surg Pathol. 1999;23:159–65.
24. Rooper LM, Bishop JA, (2020) Soft tissue special issue: adamantinoma-like ewing sarcoma of the head and neck: a practical review of a challenging emerging entity. Head Neck Pathol 14:59–69
25. Rooper LM, Jo VY, Antonescu CR, Nose V, Westra WH, et al. Adamantinoma-like ewing sarcoma of the salivary glands: a newly recognized mimicker of basaloid salivary carcinomas. Am J Surg Pathol. 2019;43:187–94.
26. Bishop JA, Alaggio R, Zhang L, Seethala RR, Antonescu CR. Adamantinoma-like Ewing family tumors of the head and neck: a pitfall in the differential diagnosis of basaloid and myoepithelial carcinomas. Am J Surg Pathol. 2015;39:1267–74.
27. Weinreb I, Goldstein D, Perez-Ordoñez B. Primary extraskeletal Ewing family tumor with complex epithelial differentiation: a unique case arising in the lateral neck presenting with Horner syndrome. Am J Surg Pathol. 2008;32:1742–8.
28. Ongkeko M, Zeck J, de Brito P. Molecular testing uncovers an adamantinoma-like ewing family of tumors in the thyroid: case report and review of literature. AJSP: Rev Rep. 2018;23:8–12.
29. Oliveira G, Polónia A, Cameselle-Teijeiro JM, Leitão D, Sapia S, et al. EWSR1 rearrangement is a frequent event in papillary thyroid carcinoma and in carcinoma of the thyroid with Ewing family tumor elements (CEFTE). Virchows Arch. 2017;470:517–25.
30. McCuiston A, Bishop JA. Usefulness of NKX2.2 immunohistochemistry for distinguishing ewing sarcoma from other sinonasal small round blue cell tumors. Head Neck Pathol. 2018;12:89–94.